# On the role of rheological memory for convection driven plate-reorganizations

Lukas Fuchs[1] and Thorsten Wolfgang Becker[2]

[1]Goethe University Frankfurt
[2]University of Texas at Austin

November 30, 2022

**Abstract**

Understanding the temporal variability of Earth's tectonics is key to unraveling how mantle convection transports heat. The stability of plate motions depends on rheological "memory", i.e., the persistence of weak zones. Here, we analyze the impact of such memory in global, oceanic-lithosphere only models of visco-plastic mantle convection. Self-consistently formed weak zones are reactivated in distinct modes, and convection selects pre-damaged zones preferentially for new plate boundaries. Any local stabilizing effects of weakening are overwhelmed statistically by the accumulation of rheological heterogeneity. Reactivation of damage zones increases the frequency of plate reorganizations and thus reduces the dominant period of heat loss fluctuations. In nature, the generation of sutures may thus counteract and possibly overcome the effects of reduced convective vigor throughout planetary cooling, with implications for the frequency of orogeny and convective transport throughout Wilson cycles.

L. Fuchs[1] and T.W. Becker[2,3,4]

[1]Institute for Geosciences, Goethe University, Frankfurt/Main, Germany.

[2]Institute for Geophysics, Jackson School of Geosciences, The University of Texas at Austin, Austin, Texas, USA.

[3]Department of Geological Sciences, Jackson School of Geoscience, The University of Texas at Austin, Austin, Texas, USA.

[4] Oden Institute for Computational Engineering and Sciences, The University of Texas at Austin, Austin, Texas, USA

Corresponding author: Lukas Fuchs (fuchs@geophysik.uni-frankfurt.de)

Key Points:

- Results from global, plate generating convection models with damage
- Rheological memory leads to reactivation of sutures and enhanced plate reorganizations
- 30% reduction in heat transport cyclicity counteracts decrease in convective vigor

Abstract

Understanding the temporal variability of Earth's tectonics is key to unraveling how mantle convection transports heat. The stability of plate motions depends on rheological "memory", i.e., the persistence of weak zones. Here, we analyze the impact of such memory in global, oceanic-lithosphere only models of visco-plastic mantle convection. Self-consistently formed weak zones are reactivated in distinct modes, and convection selects pre-damaged zones preferentially for new plate boundaries. Any local stabilizing effects of weakening are overwhelmed statistically by the accumulation of rheological heterogeneity. Reactivation of

damage zones increases the frequency of plate reorganizations and thus reduces the dominant period of heat loss fluctuations. In nature, the generation of sutures may thus counteract and possibly overcome the effects of reduced convective vigor throughout planetary cooling, with implications for the frequency of orogeny and convective transport throughout Wilson cycles.

## 1 Introduction

Within our solar system, plate-tectonics is unique among the terrestrial planets and key for the thermal evolution of the entire Earth. The motions and reorganization of oceanic plates is part of the cold, surface boundary layer of mantle convection (Turcotte & Oxburgh, 1967), and embedded within are the creation and recycling of continents throughout the supercontinental cycle (e.g., Wilson, 1966). However, how the interactions between oceanic and continental systems serve to control both the long-term trends and fluctuations of tectonic activity and heat transport remains debated (e.g., Condie et al., 2015; Mitchell et al., 2021).

To form plate boundaries, high lithospheric strength as expected from temperature-dependent viscosity needs to be overcome (e.g., Moresi & Solomatov, 1998), and plastic yielding produces broadly plate-like surface planforms in global convection models (e.g., van Heck & Tackley, 2008; Foley & Becker, 2009). However, such models require yield stresses that are low compared to expectations from rock mechanics. Moreover, one possibly important ingredient, the memory of past deformation, has so far been missing from global models. It is this memory effect of tectonic damage on which we focus here.

Supercontinental assembly and break-up throughout the Wilson cycle leave behind a deformed surface which can sustain weakened regions for perhaps longer than $10^9$ years (e.g., Burke et al., 1977; Sykes, 1978; Buiter & Tosvik, 2014). Such sutures, or damage zones, significantly differ from the surrounding lithosphere, e.g., compositionally or mechanically, such as due to failed rifts. Sutures represent rheological "memory" which can then be recalled, for example for subduction initiation (e.g., Gurnis et al., 2000; Crameri et al., 2020). Given that continental plates record geology for ˜10 times longer than the more rapidly recycled oceanic lithosphere, memory effects will be most important for the continents.

However, even if the lithosphere were purely oceanic, memory will matter, for example because the formation of plate boundaries is connected to the processes that reduce brittle or plastic strength with sustained deformation in the first place, i.e., strain weakening and localization. While sphericity and high convective vigor appear to produce ridge offsets for visco-plastic convection (Langemeyer et al., 2021), it is typically held that deformation-dependent strength is required to explain hallmarks of plate tectonics (e.g., Bercovici, 1993). Which micro-physical mechanisms serve to localize deformation (e.g., Montesi, 2013) and if an isotropic description is sufficient (e.g., Tommasi & Vauchez, 2001) has long been debated. However, grainsize-dependence is one promising candidate for plate boundaries (e.g., Bercovici & Ricard, 2016), and the controls on damage creation and healing have far-reaching implications for planetary evolution (e.g., Foley & Driscoll, 2016).

Simplified descriptions based on tracking an evolving damage variable can capture much of the more complex hysteresis due to grain-size dependence (Fuchs & Becker, 2021), and such approximations are more readily explored within convection models (e.g., Tackley 2000c, Ogawa, 2003). Here, we build on the 2-D modeling of Fuchs & Becker (2019) and explore, to our knowledge for the first time, the effects of memory on global, visco-plastic convection. While we explore an idealized, oceanic plate only system at reduced convective vigor compared to the Earth, for simplicity, interesting behavior arises that allows us to speculate on the role of damage for plate tectonics.

## 2 Methods

### 2.1 Model Setup

All computations were performed in a spherical shell using *CitcomS* (Moresi & Solomatov, 1995; Zhong et al., 2000; Tan et al., 2006), a well-benchmarked finite element code that solves the equations for conservation of mass, momentum, and energy in a fluid under the Boussinesq approximation:

Here $u$ is velocity, $P$ dynamic pressure, $\eta$viscosity, $T$ temperature, and $H_T$ internal heat production. The term $X_{,y}$ stands for the derivative of $X$ in the direction of $y$ , where $i$ and$j$ are the spatial indices, $r$ is the radial direction, and$t$ represents time (e.g., Zhong et al., 2000). The system is heated purely internally with a constant rate of non-dimensionalized heat production ($H_T = 60$, which scales to ˜ 7 TW), where we assume zero heat flux and free slip at the bottom and a constant temperature ( $T = 0$) and free slip at the top. Pure internal heating excludes plumes as sources of plate reorganization (e.g., Foley & Becker, 2009; Arnould et al., 2020), again for simplicity.

The Rayleigh number is typically defined as

where $\rho$ , $g$ , $\alpha$ , $\Delta T$ , $R$ ,$\eta_{\rho\epsilon\varphi}$ and $\kappa$ are the density, gravitational acceleration, thermal expansion, temperature difference across the convecting layer, radius of the Earth, reference viscosity, and thermal diffusivity, respectively. All parameters are non-dimensional using$R$ as the length scale (Zhong et al., 2000). To compare the convective vigor, one can also consider the mantle thickness, $D$ , for the Rayleigh number:

.

As we use internal heating, one should also consider the internal heating Rayleigh number which is defined as:

,

where $r$ is the ratio of the outer core radius over the radius of the Earth. All parameters as used are summarized in Table S1. From eqs. - , $Ra$ is in the range of $10^7$ - $10^9$.

### 2.2 Rheology

The temperature-dependence of viscosity is described by an Arrhenius-type relationship (e.g., Tackley, 2000b, c) for the non-dimensional viscosity

,

where $T$ is the non-dimensional temperature (scaled by temperature difference $\Delta T$ ), $\eta_\epsilon$ is the non-dimensional activation energy (23.03). Our parameters result in a total viscosity variation of 5 orders of magnitude. This is a moderate viscosity contrast with respect to what is expected for Earth. However, visco-plastic convection with such viscosity ranges results in plate-like surface motions (e.g., van Heck & Tackley, 2008; Foley & Becker, 2009). While our models are thus not quite Earth-like, we consider them meaningful as a reference from which we explore the role of strain-dependent weakening and hardening (SDWH).

The strength of the material is defined by its yield stress (e.g., Tackley, 2000a, c):

,

where $a$ is the cohesion, $b$ is the depth gradient. This can describe a failure envelope for 'brittle' behavior in shallow depths, where $z$ is the depth, and $\lambda$ is a constant yield stress for 'ductile' behavior. SDWH rheology can capture damage memory within the upper thermal boundary layer of thermal convection. We explore the temporal evolution of a quasi-strain, $\gamma$ , that plays the role of a damage variable as (e.g., Gerya, 2013; Tackley, 2000b):

,

where is the second invariant of the strain rate tensor, $T$ the temperature, and $H$ the temperature-dependent healing rate defined as (e.g., Tackley, 2000b):

.

Here, $B$ is the healing time scale and $\eta_\gamma$ a nondimensional activation energy. Thus, for a high (low)$\eta_\gamma$ the healing term depends more (less) on temperature, and $B$ governs the hardening rate within the mantle (e.g.,

Fuchs & Becker, 2019). This somewhat *ad-hoc* description can be viewed as an abstraction and constraint on the actual micro-physics (e.g., Fuchs & Becker, 2021), and we choose values for $B$ and $\eta_\gamma$ which result in similar (and slower) hardening rates compared to a single mineral phase, composite, grain-size sensitive rheology (cf. Hirth & Kohlstedt, 2003; Behn et al., 2009; see supplementary text S1 for more details).

Different combinations of SDWH have been proposed. Here, we assume that a linear reduction of the yield stress due to $\gamma$ , i.e., plastic-strain softening (PSS), results in rheological weakening. Plastic-strain softening best approximates the behavior of a grain-size sensitive (GSS), composite rheology (Fuchs & Becker, 2021). While we limit the rheological weakening and hardening rates described by the SDWH parameters to the transient behavior of GSS rheology, additional microphysical mechanisms might be used as further constraints.

The effective yield stress is defined as (e.g., Lavier et al., 2000):

,

where $D_{max}$ is the maximum damage and $\gamma_{S\rho}$ (10) is the critical strain for which maximum damage is reached. The amplitude of $\gamma$ governs the intensity of weakening, while healing leads to rheological hardening due to the increase of the yield stress. The yield and effective viscosity are then defined as (e.g., Tackley, 2000b, c):

.

### 2.3 Modelling approach and diagnostics

For our reference model without SDWH, we chose a Rayleigh number, yield stress, and yield stress depth-gradient that is close to the transition to episodic-lid convection (cf. Foley & Becker, 2009) and subsequently increase the yield stress and its gradient. Our parameter combination leads to the most plate-like character (for our assumptions), i.e., strong subducting slabs, and no yielding within the lower mantle. We then systematically vary the healing parameters $B$ and $\eta_\gamma$ to increase the rheological memory within the lithosphere and mantle and focus on the results from ˜30 models here. All start from a mobile-lid stage and ran for a period of at least 75 overturn times (OT). One overturn time is defined as the ratio of twice the thickness of the mantle divided by the time average of the root-mean square velocity of the model, corresponding to ˜200 Myr for Earth.

We proceed to discuss the surface patterns of the effective viscosity and second strain-rate tensor invariant as well as depth slices of the effective viscosity (Figure 1), to determine the effect of SDWH on the convective vigor, the surface dynamics and plate reorganizations. To extract quantitative bulk behavior metrics, we focus on time-averages of the surface-averaged effective viscosity ¡$\eta_{\text{surf}}/\eta_0$ ¿, the relative area of inherited weak zones (IWZs) ¡$A_{ID/HD}$ ¿, as well as the dominant period $T_{dom}$ of the total surface heat flux $Q_{surf}$ (see supplementary text S2 for more details). The relative area of IWZs, $A_{ID/HD}$ , quantifies the amount of presently non-deforming lithospheric IWZs relative to the entire, highly deformed areas (e.g., active subduction zones or high strain-rate spreading centers). The dominant period of $Q_{surf}$ provides a good first-order approximation on the cyclicity of plate reorganizations. For the time-averaged metrics we do discuss, we calculate the median of the full time series of each model, starting at a minimum time of 20 OT to avoid initial condition effects.

To quantify the intensity of SDWH, we calculated the average lithospheric damage ¡$\gamma_\Lambda$ ¿ via the depth-integral of the quasi-strain along a volumetrically averaged radial profile, considering only the upper thermal boundary layer normalized by $Z$ . The ¡$\gamma_\Lambda$ ¿ metric provides a good overall estimate on the effectiveness of SDWH and we use ¡$\gamma_\Lambda$ ¿ as the control parameter subsequently. The absolute healing rate at the surface and its temperature-dependence within the upper thermal boundary layer mainly control the weak zones dynamics, as might be expected, and ¡$\gamma_\Lambda$ ¿ can also capture this behavior to first order.

In the following, we describe the effect of a SDWH rheology on the convective planform and dynamics, in particular the time-dependence of plate reorganization. We first describe different types of IWZ reactivations

which are characteristic features of our models (Figure 1) followed by a description of the global effect of strain weakening and rheological memory.

3 Results

### 3.1 Reactivation of inherited weak zones

Depending on the longevity of memory (governed by $B$ and$\eta_\gamma$ ), damage accumulation and preservation is effective to form IWZs within the lithosphere (Figure S1). The intensity of those IWZs as well as their contrast to the adjacent lithosphere is governed by the SDWH rheology. There are a range of surface healing rates, $H_{Surf}$ , for which no IWZs are formed ($H_{Surf}$ $> 10^3$). Weak zones are short lived and can not be reactivated for slightly smaller healing rates ($H_{Surf}$ ~ $10^2$ – $10^3$). Pronounced IWZ are observed for intermediate rates ($H_{Surf}$ $= 10^{-1}$ - $10^3$) in combination with a wide range of temperature-dependence, governed by $\eta_\gamma$ (i.e., a longer damage memory with depth, e.g., quantifiable via the depth-integral of $\gamma$ or $H$ ). For$H_{Surf}$ ~ $10^{-1}$ - $10^2$, IWZs can be reactivated (Figure 1). For even smaller $H_{Surf} < 10^{-1}$, weakening of the lithosphere becomes too intense, resulting in more frequent reorganization of plate motions, due to easier yielding resulting in overall higher convective vigor.

Well-pronounced weak zones form due to the continuous deformation along convergent (subduction) zones, enabling a kind of lubrication layer. This becomes apparent once the slab breaks off (highlighted by the dark contour lines in the surface plots of Figure 1). The IWZs are transported laterally with the lithosphere and are then either subducted along existing convergent boundaries, cut up and dispersed by migrating divergent boundaries, or reactivated as new plate boundaries, both in divergent and convergent margins. This effect is partly controlled by$\eta_\gamma$ , as it controls the depth extent of the weak zone through the lithosphere, similar to what was explored in 2-D by Fuchs and Becker (2019). However, a quantification of the required weakening intensity as well as depth penetration for reactivation is less straight forward, mainly due to the additional degrees of freedom provided by 3-D flow.

For pronounced IWZs, two different types of reactivations are observed. Figure 1 shows an example with both types; the initial IWZs are highlighted by the red square in the surface plots. An IWZ may serve as, 1), a lateral guide for propagating convergent boundaries (e.g., Figure 1, southern IWZ, marked with a green triangle), e.g., such that an active subduction zone grows laterally. This kind of reactivation is observed frequently within the models and is facilitated by the lower yield stress within the IWZ with respect to the surrounding lithosphere (best seen by the contour lines of the IWZ area in the surface plots).

A less frequently observed reactivation is, 2), the formation of a new convergent boundary (e.g., Figure 1, northern IWZ, marked with a red triangle). Such reactivation happens when the IWZ lies within a plate that is under external compression, such as divergent boundaries around their edges, akin to the setting of, e.g., present-day Antarctica. The IWZ has a lower yield stress than the adjacent lithosphere and due to the increasing thickening of the top thermal boundary layer in a compressional stage, further weakening occurs within the IWZ (see the decrease in the effective viscosity along the northern IWZ, Figure 1) until a new convergent boundary is formed. Type 2) reactivation depends on the large-scale plate dynamics and a well-established IWZ. Reactivation via a new convergent boundary is less frequent than reorganization via lateral propagation; models with continental lithosphere that is recycled more slowly may make this scenario more likely. IWZs are also reactivated as divergent boundaries. Again, reactivation via a lateral extension of an active boundary (type 1) is observed more frequently than through the formation of a new divergent boundary (type 2).

In case of stronger weakening and longer damage memory, reorganization happens more frequently due to the increasingly more pervasively weakened lithosphere as reorganized by subduction. Such models do not show the type 2 IWZ reactivations. Weak zones still serve as guides for laterally propagating subduction zones, but tend to be shorter and, thus, do have a reduced survival rate. A summary of different IWZs reactivation scenarios over the entire range of parameters explored is shown in Figure S2, and more detailed time sequences of each reactivation type in Figures S3-S6.

Based on the reactivation behavior of IWZs, we can assign each model a class with a characteristic convection pattern, surface dynamics, and weak zone reactivation. The first class is defined by models which form IWZs. However, they either harden quickly, or show no reactivation, due to less pronounced weak zones (marked as squares and lower triangles in Figure 2). The second class of models does form distinct IWZs which can be reactivated in type 1 and 2 scenarios (circles). The third class is defined by models with significant overall weakening of the lithosphere; they have short IWZ as well as weak sinking slabs, leading to a more frequent formation and destruction of convergent plate boundaries (pentagrams). The last class of models have intense weakening preventing the formation of weak zones with large strength contrast and thus also have a reduced reactivation ability (hexagrams). The weak zones in those models tend to be destroyed by subduction instead of being reactivated. This classification correlates with ¡$\gamma_A$ ¿ and thus lithospheric strength and is also predictive for the average surface damage ¡$\gamma_S$ ¿ (color scale in Figures 2, S7, and S8) or the volumetric damage ¡$\gamma$ v¿.

### 3.2 Damage weakening and memory effect

The classification of reactivation behavior correlates with other surface metrics (Figure S7). The effective surface viscosity ¡$\eta$ surf/$\eta_0$ ¿, for example, results from the accumulated damage (eqs. 9-13) and thus correlates with the reactivation behavior. With increasing memory, ¡$\gamma_A$ ¿ increases, resulting in a linear decrease of ¡$\eta$ surf/$\eta_0$ ¿. This is due to the shallow lithosphere being continuously at the yielding stress. Once ¡$\gamma_A$ ¿ surpasses ˜ 45% (equivalent to ¡$\gamma_S$ ¿ ˜ 5), reactivation switches to a more dynamic behavior. Convective vigor increases as seen from the volumetric and surface RMS velocity increase. Due to an increased convective vigor and the weakened, laterally more heterogeneous lithosphere, reorganization of the plates becomes more frequent, eventually leading to more drip-like convection. The reduction of the effective viscosity contrast between the surface and the interior results in a decrease in plateness and toroidal-poloidal ratio of the surface velocities (Figures S8a and b). However, due to a faster convection and thus more effective heat transport, the average temperature and mobility decrease (Figures S8c and d).

To distinguish between the average and amount of inherited damage within the lithosphere, we determine the relative area of IWZs of the high-damage surface area for each model via eq. (S.2) (Figure 2a). For models with fast hardening and thus not reactivating IWZs, ¡$A_{ID/HD}$ ¿ covers up to 20 % of the total high-damage area. The remaining area is described by active plate boundaries. With increasing ¡$\gamma_A$ ¿ (or ¡$\gamma_S$ ¿, or damage memory), the relative amount of IWZ area increases up to ˜ 40 %. That is, more IWZs are formed with a potentially higher longevity. Still, due to the complexities of convection, the time variation of the relative area of IWZs remains rather large (0 - 65 %). Over the entire model period there exist shorter periods in which IWZs dominate the high-damage areas and periods with almost no IWZ at all. This could be due to our oceanic lithosphere only setting, which means continuous recycling of the lithosphere. The presence of more buoyant continental lithosphere would most likely reduce the time variability of the IWZ area. However, the overall trend of an increasing area of IWZs should remain, due to frequent breakup and assemblage of continental lithosphere.

With increasing ¡$\gamma_A$ ¿, the relative IWZ area plateaus, and remains ˜steady for high ¡$\gamma_A$ ¿. A faster general yielding due to an increased overall weakened lithosphere results in more convergent boundaries and thus a larger high damage as well as actively deforming area. The rate of increase for both areas is high for a low ¡$\gamma_A$ ¿ and decreases again. At the same time, no additional IWZs are formed (i.e., the total area of IWZs remains ˜constant). More intense weakening focuses convective motions within convergent boundaries and partly stabilizes them; this effect also counteracts the formation of new IWZs. An overall more damaged lithosphere, however, results in a less effective strength contrast between existing IWZ and the adjacent lithosphere as well as in less stable slabs; this also limits the total high-damage area. Thus, the relative amount of IWZs stagnates and slightly decreases again. For our models, the area of high damage is always less than ˜ 5% and the area of IWZs is only ˜ 1.3% of the total surface area.

### 3.3 Time dependence of plate-reorganizations

The formation and destruction of convergent and divergent boundaries can be quantified by the resulting

changes in seafloor age or $Q_{Surf}$ . While the mean $Q_{Surf}$ must equal the internal heat production rate, high temporary flux corresponds to periods in which convergent boundaries are dominant, akin to the continental drift phase of the Wilson cycle. Low $Q_{Surf}$ indicates that subduction zones dominate, as it would be the case for continent assembly phase. IWZs facilitate more frequent formation of convergent boundaries; this should lead to a decrease in the dominant period of heat flow fluctuations due to the SDWH rheology. The dominant periods of $Q_{Surf}$ variation in our models can capture aspects of such plate-reorganization cyclicity changes.

With an increasing ¡$\gamma_\Lambda$ ¿ the dominant period of heat flow variations is indeed found to decrease (Figure 2b), meaning that increased damage memory leads to more frequent plate reorganization. The period decreases from ˜ 3.2 OT (i.e., ˜612 Myr for an average plate velocity of 3 cm/a) to ˜ 2.3 OT (˜440 Myr) for a model with maximum damage memory. Such a decreasing trend in the dominant period is also visible in the surface and volumetric velocities confirming more frequent variation in plate-reorganization.

A cross correlation analysis between the variability of $Q_{Surf}$ and the area of IWZs shows that there is a phase shift corresponding to a delay of ˜ 0.6 OT (˜114 Myr). That is, the area of IWZs is maximum after a maximum of $Q_{Surf}$ (i.e., the divergent boundary dominating period). The delay increases slightly for increasing ¡$\gamma_\Lambda$ ¿ up to ˜1.5 OT (˜287 Myr) for a ¡$\gamma_\Lambda$ ¿ = 0.5 and decreases again towards its mean value of ˜0.6 OT. This highlights that there is an increase in the formation of IWZs due to damage memory in the lithosphere in addition to a higher longevity of the IWZs. Reactivation as well as the stabilization of convergent boundaries (i.e., less frequent formation of new IWZs) reduce the total amount of IWZs which results in a decrease of the correlation with respect to $Q_{Surf}$ .

## 4 Discussion

The introduction of damage rheology and strain-dependent weakening in 3-D spherical, plate-like convection models shows that such an extension indeed leads to suture-like zones of persistent weakness. Those affect plate boundary stability, and often, these weak zones are reused for new plate boundaries, similar to what was found by Fuchs and Becker (2019). Progressively, this leads to a lithosphere that is more readily broken, and hence more frequent plate reorganizations with a reduction of the dominant periods of heat transport by up to ˜30%.

Plate tectonic is thus less stable with damage memory in our models than without, unlike what might be expected. Locally, plate boundaries do appear more long-lived, and the degree of shorter period power in the spectrum of heat loss is somewhat reduced for increasingly damaged models, implying some damping of fluctuations. However, we did not find robust metrics for documenting those stabilizing effects, and general time-dependence of any metrics seem to dwarf the signal. The same is true for other bulk metrics, like toroidal-poloidal ratios, which were comparable across models, and no features such as transform faults arose after inclusion of damage. This might be because our rheological description lacks strong weakening and a brittle domain, and other damage rheologies might behave differently.

Given the limitation of our models, in particular the omission of longer-lived continental lithosphere, we expect that our estimates of the extent of the suture saturation area (˜20%), and perhaps also the shift in dominant periods of heat transport (˜30%), to be underestimates of the actual role of rheological memory for the thermal evolution of the planet. When scaled to the Earth, the dominant periods of heat flux are of the same order as those suggested for supercontinental cycles, ˜500 Myr (e.g., Condie et al., 2015; Mitchell et al., 2021) though we do, of course, expect feedbacks between continental cover and the cyclicities driven by oceanic lithosphere recycling (e.g., Rolf et al., 2014). It is more meaningful to compare the relative change over Earth's evolution, for example considering indications that the inferred supercontinental periodicity has decreased by ˜50% since ˜2 Ga, and that this was accommodated by an increase in plate speeds and collision frequency (Condie et al., 2015).

Such an increase in reorganization speeds is at odds with a simple convective understanding of plate speeds which should scale as $Ra^{2/3}$ implying a reduction due to the decrease in internal heating of perhaps ˜30% since 2 Ga. Thermo-chemical convection modifies these heat flow scalings, and convective efficiency and thermal

self-regulation of plate tectonics remain debated (e.g., Korenaga, 2006; Condie et al., 2015). However, our results suggest that the generation of an ever more heterogeneous lithosphere may provide a mechanism to counterbalance and perhaps overcome the effect of reduced convective vigor over geological time.

We assume a constant healing rate over the model period, which is not the case in nature. Potentially driven by mineralogical transformation (different grain growth rates and weakening abilities), or due to the continuous secular cooling of the planet, the healing rate within the lithosphere might also decrease over time, i.e., the damage memory increases. Thus, a longer damage memory with increasing age of the Earth would result in an increase in ¡$\gamma_\Lambda$ ¿, which would lead to an even more frequent reorganization of plates and increase in orogenic activity. If healing and damage are controlled by the surface conditions (cf. Foley & Driscoll, 2016), then healing might be constant for Earth. Either way, it seems promising to factor in the evolution of the distribution of damage zones into thermal evolution models.

## 5 Conclusions

Global, visco-plastic convection models with damage allow us to begin to explore the relevance of inherited weak zones for plate reorganization in a dynamically consistent fashion. Reactivation of sutures for plate reorganizations are well documented for the Cenozoic (e.g., Crameri et al., 2020) and our models show similar reactivation patterns, as well as a ˜30% decrease in the dominant period of convective heat transport. When interpreted in terms of the long-term evolution and creation of sutures during the operation of plate tectonics, this suggest that rheological damage accumulation is contributing to the suggested increase in supercontinental and orogenic frequency since the Proterozoic (Condie et al., 2015). More generally, our models and subsequent refinements will allow deriving statistical descriptions of plate tectonic metrics as linked to internal and surface thermo-mechanical dynamics. Such work will contribute to better plate reconstructions and an enhanced understanding of terrestrial planetary evolution.

## Acknowledgements

TWB was partially support through NSF EAR 1853856 and 2121666. We use the color maps from Crameri (2018).

## Data and Software Availability Statement

Surface plots are drawn using the Generic Mapping Tools (GMT, www.soest.hawaii.edu/gmt/). The mantle convection code *CitcomS* is available at https://geodynamics.org/resources/citcoms. All model input parameters are given in Tables S1. All model input files as well as the postprocessed data and the MATLAB scripts to reproduce the surface plots and the box whisker plots will be made available as an open access dataset via *zenodo* .

## References

Arnould, M., Coltice, N., Flament, N., & Mallard, C. (2020). Plate tectonics and mantle controls on plume dynamics. *Earth and Planetary Science Letters, 547* , 116439.

Behn, M. D., Hirth, G., & Elsenbeck II, J. R. (2009). Implications of grain size evolution on the seismic structure of the oceanic upper mantle. *Earth and Planetary Science Letters, 282(1-4)* , 178-189.

Bercovici, D. (1993). A simple model of plate generation from mantle flow. *Geophysical Journal International, 114* (3), 635-650.

Bercovici, D., & Ricard, Y. (2016). Grain-damage hysteresis and plate tectonic states. *Physics of the Earth and Planetary Interiors, 253* , 31-47.

Buiter, S. J., & Torsvik, T. H. (2014). A review of Wilson Cycle plate margins: A role for mantle plumes in continental break-up along sutures?. Gondwana Research, 26(2), 627-653.

Burke, K., Dewey, J. F., & Kidd, W. S. (1977). World distribution of sutures—the sites of former oceans. *Tectonophysics, 40* (1-2), 69-99.

Condie, K., Pisarevsky, S. A., Korenaga, J., & Gardoll, S. (2015). Is the rate of supercontinent assembly changing with time?*Precambrian Research, 259* , 278-289.

Crameri, F. (2018). Scientific colour maps: perceptually uniform and colour-vision. *Zenodo* . doi:https://doi.org/10.5281/zenodo.1243862

Crameri, F., Magni, V., Domeier, M., Shephard, G. E., Chotalia, K., Cooper, G., & ... & Thielmann, M. (2020). A transdisciplinary and community-driven database to unravel subduction zone initiation.*Nature communications, 11* (1), 1-14.

Foley, B. J., & Driscoll, P. E. (2016). Whole planet coupling between climate, mantle, and core: Implications for rocky planet evolution.*Geochemistry, Geophysics, Geosystems, 17* (5), 1885-1914.

Foley, B., & Becker, T. (2009). Generation of plate-like behavior and mantle heterogeneity from a spherical, viscoplastic convection model.*Geochemistry, Geophysics, Geosystems, 612* , 18-25.

Fuchs, L., & Becker, T. W. (2019). Role of strain-dependent weakening memory on the style of mantle convection and plate boundary stability.*Geophysical Journal International, 218(1)* , 601-618.

Fuchs, L., & Becker, T. W. (2021). Deformation memory in the lithosphere: A comparison of damage-dependent weakening and grain-size sensitive rheologies. *Journal of Geophysical Research: Solid Earth, 126* (1), e2020JB020335. doi:10.1029/2020JB020335

Gerya, T. V. (2013). Initiation of transform faults at rifted continental margins: 3D petrological-thermomechanical modeling and comparison to the Woodlark Basin. *Petrology, 21(6)* , 550-560.

Gurnis, M., Zhong, S., & Toth, J. (2000). On the competing roles of fault reactivation and brittle failure in generating plate tectonics from mantle convection. In R. G. M.A. Richards (Ed.), *The History and Dynamics of Global Plate Motions* (pp. 73-94). American Geophysical Union.

Hirth, G., & Kohlstedt, D. (2003). Rheology of the upper mantle and the mantle wedge: A view from the experimentalists. *Geophysical monograph-american geophysical union, 138* , 83-106.

Korenaga, J. (2006). Archean geodynamics and the thermal evolution of Earth. *Geophysical Monograph-American Geophysical Union, 164* , 7.

Langemeyer, S. M., Lowman, J. P., & Tackley, P. J. (2021). Transform offsets occurring along divergent plate boundaries in global mantle convection models. *Communications Earth and environment, 2* , 69.

Lavier, L., Buck, W., & Poliakov, A. N. (2000). Factors controlling normal fault offset in an ideal brittle layer. *Journal of Geopysical Research: Solid Earth, 105* (B10), 23431-23442.

Mitchell, R. N., Zhang, N., Salminen, J., Liu, Y., Spencer, C. J., Steinberger, B., Murphy, J.B., Li, Z. X. (2021). The supercontinent cycle. *Nature Reviews Earth & Environment, 2* (5), 358-374.

Moresi, L. N., & Solomatov, V. S. (1995). Numerical investigation of 2D convection with extremely large viscosity variations. *Physics of Fluids, 7(9)* , 2154-2162.

Moresi, L., & Solomatov, V. (1998). Mantle convection with a brittle lithosphere: thoughts on the global tectonic styles of the Earth and Venus. *Geophysical Journal International, 133* (3), 669-682.

Ogawa, M. (2003). Plate-like regime of a numerically modeled thermal convection in a fluid with temperature-, pressure-, and stress-history-dependent viscosity. *Journal of Geophysical Research: Solid Earth, 108* (B2).

Rozel, A., Ricard, Y., & Bercovici, D. (2011). A thermodynamically self-consistent damage equation for grain size evolution during dynamic recrystallization. *Geophysical Journal International* , *184* (2), 719-728.

Sykes, L. R. (1978). Intraplate seismisity, reactivation of preexisting zones of weakness, alkaline magmatism, and other tectonism postdating continental fragmentation. *Reviews of Geophysics, 16* (4), 621-688.

Tackley, P. J. (2000a). Self-consistent generation of tectonics plates in time-dependent, three-dimensional mantle convection simulations: 1. Pseudoplastic yielding. *Geochemistry, Geophysics, Geosystems, 1* (8).

Tackley, P. J. (2000b). Self-consistent generation of tectonics plates in time-dependent, three-dimensional mantle convection simulations: 2. Strain weakening and asthenosphere. *Geochemistry, Geophysics, Geosystems, 1* (8), 1026.

Tackley, P. J. (2000c). The quest for self-consistent generation of plate tectonics in mantle convection models. *Geophysical Monograph-American Geophysical Union, 121* , 47-72.

Tan, E., Choi, E., Thoutireddy, P., Gurnis, M., & Aivazis, M. (2006). GeoFramework: Coupling multiple models of mantle convection within a computational framework. *Geochemistry, Geophysics, Geosystems, 7(6)* .

Tommasi, A., & Vauchez, A. (2001). Continental rifting parallel to ancient collisional belts: an effect of the mechanical anisotropy of the lithospheric mantle. *Earth and Planetary Science Letters, 185* (1-2), 199-210.

Turcotte, D. L., & Oxburgh, E. R. (1967). Finite amplitude convective cells and continental drift. *Journal of Fluid Mechanics, 28* (1), 29-42.

van Heck, H. J., & Tackley, P. J. (2008). Planforms of self-consistently generated plates in 3D spherical geometry.*Geophysical Research Letters, 35* (19).

Wilson, J. T. (1966). Did the Atlantic close and then re-open?*Nature, 211* , 676-681.

Zhong, S., Zuber, M. T., Moresi, L., & Gurnis, M. (2000). Role of temperature-dependent viscosity and surface plates in spherical shell models of mantle convection. *Journal of Geophysical Research: Solid Earth, 105* (B5), 11063-11082.

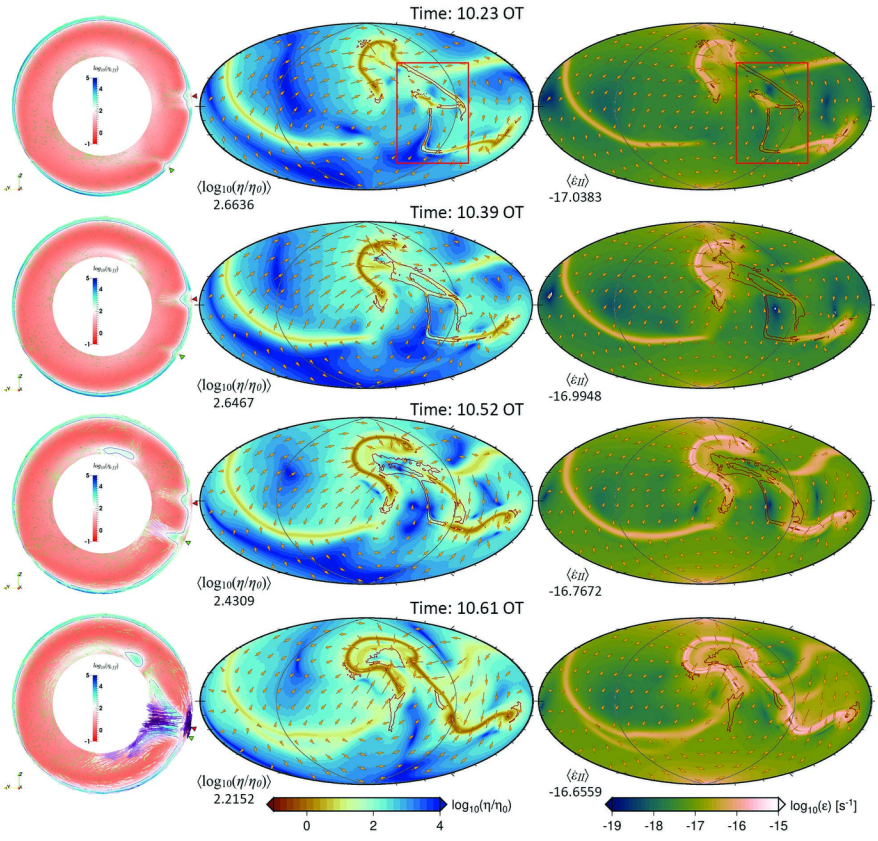

**Figure 1** . Inherited weak zone reactivation. Snapshots of reactivations of inherited weak zones (IWZs) in a model with strain-dependent weakening parameters of $B = 2.44[?]10^9$ and $\eta_\gamma = 92.103$. Viscosity cross section (left) along the black intersection shown on the surface plots for viscosity (middle) and strain rate (right) with red contours delineating the area of IWZs following eq. (S.2). IWZs can be reactivated in two ways: 1), as guide for a laterally propagating subduction zone (south of the equator, green triangle in the cross-section), and 2), as a newly formed subduction zone (near the equator, red triangle in the cross-sections).

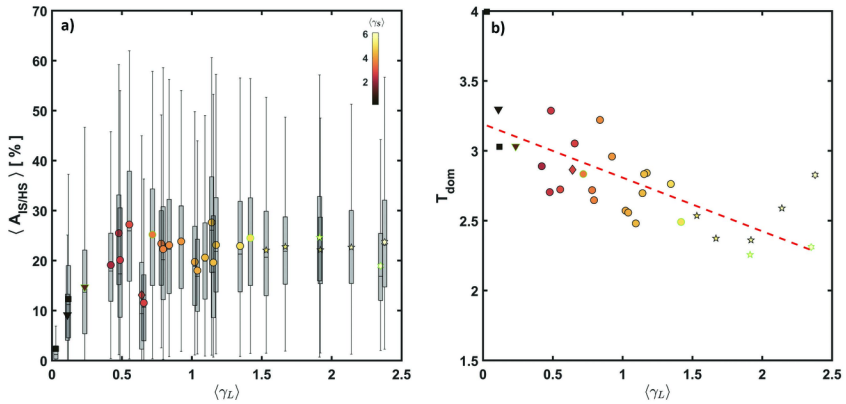


**Figure 2.** Memory effect and plate reorganization time-dependence. **a)** Relative area of inherited weak zone (IWZ);**b)** Dominant period of the total surface heat flux $Q_{surf}$ , both shown with symbols showing the median and box whisker plots for the range over model time, against the average lithospheric damage ¡$\gamma_\Lambda$ ¿. Symbol color denotes time-averaged surface damage ¡$\gamma_S$ ¿, and the dashed curve a linear fit. Symbol type denotes the reactivation behavior (diamond: reference model, no SDWH; square: no IWZ; lower triangle: formation for IWZ, but no reactivation; circle: formation of IWZ and reactivation; pentagram: formation of IWZ, strong weakening effect; hexagram: formation of IWZ, too effective weakening; see text for more details). Symbols with green edge show models from Figure S2.

**Hosted file**

`agu_suppinfo_word_oct10_21.docx` available at https://authorea.com/users/558950/articles/607852-on-the-role-of-rheological-memory-for-convection-driven-plate-reorganizations

L. Fuchs[1] and T.W. Becker[2,3,4]

[1]Institute for Geosciences, Goethe University, Frankfurt/Main, Germany.

[2]Institute for Geophysics, Jackson School of Geosciences, The University of Texas at Austin, Austin, Texas, USA.

[3]Department of Geological Sciences, Jackson School of Geoscience, The University of Texas at Austin, Austin, Texas, USA.

[4] Oden Institute for Computational Engineering and Sciences, The University of Texas at Austin, Austin, Texas, USA

Corresponding author: Lukas Fuchs (fuchs@geophysik.uni-frankfurt.de)

Key Points:

- Results from global, plate generating convection models with damage
- Rheological memory leads to reactivation of sutures and enhanced plate reorganizations
- 30% reduction in heat transport cyclicity counteracts decrease in convective vigor

Abstract

Understanding the temporal variability of Earth's tectonics is key to unraveling how mantle convection transports heat. The stability of plate motions depends on rheological "memory", i.e., the persistence of weak zones. Here, we analyze the impact of such memory in global, oceanic-lithosphere only models of visco-plastic mantle convection. Self-consistently formed weak zones are reactivated in distinct modes, and convection selects pre-damaged zones preferentially for new plate boundaries. Any local stabilizing effects of weakening are overwhelmed statistically by the accumulation of rheological heterogeneity. Reactivation of damage zones increases the frequency of plate reorganizations and thus reduces the dominant period of heat loss fluctuations. In nature, the generation of sutures may thus counteract and possibly overcome the effects of reduced convective vigor throughout planetary cooling, with implications for the frequency of orogeny and convective transport throughout Wilson cycles.

## 1 Introduction

Within our solar system, plate-tectonics is unique among the terrestrial planets and key for the thermal evolution of the entire Earth. The motions and reorganization of oceanic plates is part of the cold, surface boundary layer of mantle convection (Turcotte & Oxburgh, 1967), and embedded within are the creation and recycling of continents throughout the supercontinental cycle (e.g., Wilson, 1966). However, how the interactions between oceanic and continental systems serve to control both the long-term trends and fluctuations of tectonic activity and heat transport remains debated (e.g., Condie et al., 2015; Mitchell et al., 2021).

To form plate boundaries, high lithospheric strength as expected from temperature-dependent viscosity needs to be overcome (e.g., Moresi & Solomatov, 1998), and plastic yielding produces broadly plate-like surface planforms in global convection models (e.g., van Heck & Tackley, 2008; Foley & Becker, 2009). However, such models require yield stresses that are low compared to expectations from rock mechanics. Moreover, one possibly important ingredient, the memory of past deformation, has so far been missing from global models. It is this memory effect of tectonic damage on which we focus here.

Supercontinental assembly and break-up throughout the Wilson cycle leave behind a deformed surface which can sustain weakened regions for perhaps longer than $10^9$ years (e.g., Burke et al., 1977; Sykes, 1978; Buiter & Tosvik, 2014). Such sutures, or damage zones, significantly differ from the surrounding lithosphere, e.g., compositionally or mechanically, such as due to failed rifts. Sutures represent rheological "memory" which can then be recalled, for example for subduction initiation (e.g., Gurnis et al., 2000; Crameri et al., 2020). Given that continental plates record geology for ~10 times longer than the more rapidly recycled oceanic lithosphere, memory effects will be most important for the continents.

However, even if the lithosphere were purely oceanic, memory will matter, for example because the formation of plate boundaries is connected to the processes that reduce brittle or plastic strength with sustained deformation in the first place, i.e., strain weakening and localization. While sphericity and high convective vigor appear to produce ridge offsets for visco-plastic convection (Langemeyer et al., 2021), it is typically held that deformation-dependent strength is required to explain hallmarks of plate tectonics (e.g., Bercovici, 1993). Which micro-physical mechanisms serve to localize deformation (e.g., Montesi, 2013) and if an isotropic description is sufficient (e.g., Tommasi & Vauchez, 2001) has long been debated. However, grainsize-dependence is one promising candidate for plate boundaries (e.g., Bercovici & Ricard, 2016), and the controls on damage creation and healing have far-reaching implications for planetary evolution (e.g., Foley & Driscoll, 2016).

Simplified descriptions based on tracking an evolving damage variable can capture much of the more complex hysteresis due to grain-size dependence (Fuchs & Becker, 2021), and such approximations are more readily explored within convection models (e.g., Tackley 2000c, Ogawa, 2003). Here, we build on the 2-D modeling of Fuchs & Becker (2019) and explore, to our knowledge for the first time, the effects of memory on global, visco-plastic convection. While we explore an idealized, oceanic plate only system at reduced convective vigor compared to the Earth, for simplicity, interesting behavior arises that allows us to speculate on the role of damage for plate tectonics.

## 2 Methods

### 2.1 Model Setup

All computations were performed in a spherical shell using *CitcomS* (Moresi & Solomatov, 1995; Zhong et al., 2000; Tan et al., 2006), a well-benchmarked finite element code that solves the equations for conservation of mass, momentum, and energy in a fluid under the Boussinesq approximation:

Here $u$ is velocity, $P$ dynamic pressure, viscosity, $T$ temperature, and $H_T$ internal heat production. The term $X_{,y}$ stands for the derivative of $X$ in the direction of $y$, where $i$ and $j$ are the spatial indices, $r$ is the radial direction, and $t$ represents time (e.g., Zhong et al., 2000). The system is heated purely internally with a constant rate of non-dimensionalized heat production ($H_T = 60$, which scales to ~ 7 TW), where we assume zero heat flux and free slip at the bottom and a constant temperature ($T = 0$) and free slip at the top. Pure internal heating excludes plumes as sources of plate reorganization (e.g., Foley & Becker, 2009; Arnould et al., 2020), again for simplicity.

The Rayleigh number is typically defined as

where , $g$, , $\Delta T$, $R$, $_{ref}$ and are the density, gravitational acceleration, thermal expansion, temperature difference across the convecting layer, radius of the Earth, reference viscosity, and thermal diffusivity, respectively. All parameters are non-dimensional using $R$ as the length scale (Zhong et al., 2000). To compare the convective vigor, one can also consider the mantle thickness, $D$, for the Rayleigh number:

.

As we use internal heating, one should also consider the internal heating Rayleigh number which is defined as:

,

where $r$ is the ratio of the outer core radius over the radius of the Earth. All parameters as used are summarized in Table S1. From eqs. - , $Ra$ is in the range of $10^7$ - $10^9$.

### 2.2 Rheology

The temperature-dependence of viscosity is described by an Arrhenius-type relationship (e.g., Tackley, 2000b, c) for the non-dimensional viscosity

,

where $T$ is the non-dimensional temperature (scaled by temperature difference $\Delta T$), $_e$ is the non-dimensional activation energy (23.03). Our parameters result in a total viscosity variation of 5 orders of magnitude. This is a moderate viscosity contrast with respect to what is expected for Earth. However, visco-plastic convection with such viscosity ranges results in plate-like surface motions (e.g., van Heck & Tackley, 2008; Foley & Becker, 2009). While our models are thus not quite Earth-like, we consider them meaningful as a reference from which we explore the role of strain-dependent weakening and hardening (SDWH).

The strength of the material is defined by its yield stress (e.g., Tackley, 2000a, c):

,

where $a$ is the cohesion, $b$ is the depth gradient. This can describe a failure envelope for 'brittle' behavior in shallow depths, where $z$ is the depth, and is a constant yield stress for 'ductile' behavior. SDWH rheology can capture damage memory within the upper thermal boundary layer of thermal convection. We explore the temporal evolution of a quasi-strain, , that plays the role of a damage variable as (e.g., Gerya, 2013; Tackley, 2000b):

,

where is the second invariant of the strain rate tensor, $T$ the temperature, and $H$ the temperature-dependent healing rate defined as (e.g., Tackley, 2000b):

.

Here, $B$ is the healing time scale and a nondimensional activation energy. Thus, for a high (low) the healing term depends more (less) on temperature, and $B$ governs the hardening rate within the mantle (e.g., Fuchs & Becker, 2019). This somewhat *ad-hoc* description can be viewed as an abstraction and constraint on the actual micro-physics (e.g., Fuchs & Becker, 2021), and we choose values for $B$ and which result in similar (and slower) hardening rates compared to a single mineral phase, composite, grain-size sensitive rheology (cf. Hirth & Kohlstedt, 2003; Behn et al., 2009; see supplementary text S1 for more details).

Different combinations of SDWH have been proposed. Here, we assume that a linear reduction of the yield stress due to , i.e., plastic-strain softening (PSS), results in rheological weakening. Plastic-strain softening best approximates the behavior of a grain-size sensitive (GSS), composite rheology (Fuchs & Becker, 2021). While we limit the rheological weakening and hardening rates described by the SDWH parameters to the transient behavior of GSS rheology, additional microphysical mechanisms might be used as further constraints.

The effective yield stress is defined as (e.g., Lavier et al., 2000):

,

where $D_{max}$ is the maximum damage and $_{cr}$ (10) is the critical strain for which maximum damage is reached. The amplitude of governs the intensity of weakening, while healing leads to rheological hardening due to the increase of the yield stress. The yield and effective viscosity are then defined as (e.g., Tackley, 2000b, c):

.

### 2.3 Modelling approach and diagnostics

For our reference model without SDWH, we chose a Rayleigh number, yield stress, and yield stress depth-gradient that is close to the transition to episodic-lid convection (cf. Foley & Becker, 2009) and subsequently increase the yield stress and its gradient. Our parameter combination leads to the most plate-like character (for our assumptions), i.e., strong subducting slabs, and no yielding within the lower mantle. We then systematically vary the healing parameters $B$ and  to increase the rheological memory within the lithosphere and mantle and focus on the results from ~30 models here. All start from a mobile-lid stage and ran for a period of at least 75 overturn times (OT). One overturn time is defined as the ratio of twice the thickness of the mantle divided by the time average of the root-mean square velocity of the model, corresponding to ~200 Myr for Earth.

We proceed to discuss the surface patterns of the effective viscosity and second strain-rate tensor invariant as well as depth slices of the effective viscosity (Figure 1), to determine the effect of SDWH on the convective vigor, the surface dynamics and plate reorganizations. To extract quantitative bulk behavior metrics, we focus on time-averages of the surface-averaged effective viscosity $\langle {}_{\text{surf}}/{}_{0}\rangle$, the relative area of inherited weak zones (IWZs) $\langle A_{ID/HD}\rangle$, as well as the dominant period $T_{dom}$ of the total surface heat flux $Q_{surf}$ (see supplementary text S2 for more details). The relative area of IWZs, $A_{ID/HD}$, quantifies the amount of presently non-deforming lithospheric IWZs relative to the entire, highly deformed areas (e.g., active subduction zones or high strain-rate spreading centers). The dominant period of $Q_{surf}$ provides a good first-order approximation on the cyclicity of plate reorganizations. For the time-averaged metrics we do discuss, we calculate the median of the full time series of each model, starting at a minimum time of 20 OT to avoid initial condition effects.

To quantify the intensity of SDWH, we calculated the average lithospheric damage $\langle {}_{L}\rangle$ via the depth-integral of the quasi-strain along a volumetrically averaged radial profile, considering only the upper thermal boundary layer normalized by $Z$. The $\langle {}_{L}\rangle$ metric provides a good overall estimate on the effectiveness of SDWH and we use $\langle {}_{L}\rangle$ as the control parameter subsequently. The absolute healing rate at the surface and its temperature-dependence within the upper thermal boundary layer mainly control the weak zones dynamics, as might be expected, and $\langle {}_{L}\rangle$ can also capture this behavior to first order.

In the following, we describe the effect of a SDWH rheology on the convective planform and dynamics, in particular the time-dependence of plate reorganization. We first describe different types of IWZ reactivations which are characteristic features of our models (Figure 1) followed by a description of the global effect of strain weakening and rheological memory.

3 Results

### 3.1 Reactivation of inherited weak zones

Depending on the longevity of memory (governed by $B$ and  ), damage accumulation and preservation is effective to form IWZs within the lithosphere (Figure

S1). The intensity of those IWZs as well as their contrast to the adjacent lithosphere is governed by the SDWH rheology. There are a range of surface healing rates, $H_{Surf}$, for which no IWZs are formed ($H_{Surf} > 10^3$). Weak zones are short lived and can not be reactivated for slightly smaller healing rates ($H_{Surf} \sim 10^2$ – $10^3$). Pronounced IWZ are observed for intermediate rates ($H_{Surf} = 10^{-1}$ - $10^3$) in combination with a wide range of temperature-dependence, governed by (i.e., a longer damage memory with depth, e.g., quantifiable via the depth-integral of or $H$). For $H_{Surf} \sim 10^{-1}$ - $10^2$, IWZs can be reactivated (Figure 1). For even smaller $H_{Surf} < 10^{-1}$, weakening of the lithosphere becomes too intense, resulting in more frequent reorganization of plate motions, due to easier yielding resulting in overall higher convective vigor.

Well-pronounced weak zones form due to the continuous deformation along convergent (subduction) zones, enabling a kind of lubrication layer. This becomes apparent once the slab breaks off (highlighted by the dark contour lines in the surface plots of Figure 1). The IWZs are transported laterally with the lithosphere and are then either subducted along existing convergent boundaries, cut up and dispersed by migrating divergent boundaries, or reactivated as new plate boundaries, both in divergent and convergent margins. This effect is partly controlled by , as it controls the depth extent of the weak zone through the lithosphere, similar to what was explored in 2-D by Fuchs and Becker (2019). However, a quantification of the required weakening intensity as well as depth penetration for reactivation is less straight forward, mainly due to the additional degrees of freedom provided by 3-D flow.

For pronounced IWZs, two different types of reactivations are observed. Figure 1 shows an example with both types; the initial IWZs are highlighted by the red square in the surface plots. An IWZ may serve as, 1), a lateral guide for propagating convergent boundaries (e.g., Figure 1, southern IWZ, marked with a green triangle), e.g., such that an active subduction zone grows laterally. This kind of reactivation is observed frequently within the models and is facilitated by the lower yield stress within the IWZ with respect to the surrounding lithosphere (best seen by the contour lines of the IWZ area in the surface plots).

A less frequently observed reactivation is, 2), the formation of a new convergent boundary (e.g., Figure 1, northern IWZ, marked with a red triangle). Such reactivation happens when the IWZ lies within a plate that is under external compression, such as divergent boundaries around their edges, akin to the setting of, e.g., present-day Antarctica. The IWZ has a lower yield stress than the adjacent lithosphere and due to the increasing thickening of the top thermal boundary layer in a compressional stage, further weakening occurs within the IWZ (see the decrease in the effective viscosity along the northern IWZ, Figure 1) until a new convergent boundary is formed. Type 2) reactivation depends on the large-scale plate dynamics and a well-established IWZ. Reactivation via a new convergent boundary is less frequent than reorganization via lateral propagation; models with continental lithosphere that is recycled more slowly may make this scenario more likely. IWZs are also reactivated as divergent boundaries. Again,

reactivation via a lateral extension of an active boundary (type 1) is observed more frequently than through the formation of a new divergent boundary (type 2).

In case of stronger weakening and longer damage memory, reorganization happens more frequently due to the increasingly more pervasively weakened lithosphere as reorganized by subduction. Such models do not show the type 2 IWZ reactivations. Weak zones still serve as guides for laterally propagating subduction zones, but tend to be shorter and, thus, do have a reduced survival rate. A summary of different IWZs reactivation scenarios over the entire range of parameters explored is shown in Figure S2, and more detailed time sequences of each reactivation type in Figures S3-S6.

Based on the reactivation behavior of IWZs, we can assign each model a class with a characteristic convection pattern, surface dynamics, and weak zone reactivation. The first class is defined by models which form IWZs. However, they either harden quickly, or show no reactivation, due to less pronounced weak zones (marked as squares and lower triangles in Figure 2). The second class of models does form distinct IWZs which can be reactivated in type 1 and 2 scenarios (circles). The third class is defined by models with significant overall weakening of the lithosphere; they have short IWZ as well as weak sinking slabs, leading to a more frequent formation and destruction of convergent plate boundaries (pentagrams). The last class of models have intense weakening preventing the formation of weak zones with large strength contrast and thus also have a reduced reactivation ability (hexagrams). The weak zones in those models tend to be destroyed by subduction instead of being reactivated. This classification correlates with $\langle \ _L \rangle$ and thus lithospheric strength and is also predictive for the average surface damage $\langle \ _s \rangle$ (color scale in Figures 2, S7, and S8) or the volumetric damage $\langle \ _\mathrm{V} \rangle$.

### 3.2 Damage weakening and memory effect

The classification of reactivation behavior correlates with other surface metrics (Figure S7). The effective surface viscosity $\langle \ _{\mathrm{surf}/ \ 0} \rangle$, for example, results from the accumulated damage (eqs. 9-13) and thus correlates with the reactivation behavior. With increasing memory, $\langle \ _L \rangle$ increases, resulting in a linear decrease of $\langle \ _{\mathrm{surf}/ \ 0} \rangle$. This is due to the shallow lithosphere being continuously at the yielding stress. Once $\langle \ _L \rangle$ surpasses $\sim 45\%$ (equivalent to $\langle \ _s \rangle \sim 5$), reactivation switches to a more dynamic behavior. Convective vigor increases as seen from the volumetric and surface RMS velocity increase. Due to an increased convective vigor and the weakened, laterally more heterogeneous lithosphere, reorganization of the plates becomes more frequent, eventually leading to more drip-like convection. The reduction of the effective viscosity contrast between the surface and the interior results in a decrease in plateness and toroidal-poloidal ratio of the surface velocities (Figures S8a and b). However, due to a faster convection and thus more effective heat transport, the average temperature and mobility decrease (Figures S8c and d).

To distinguish between the average and amount of inherited damage within the lithosphere, we determine the relative area of IWZs of the high-damage surface area for each model via eq. (S.2) (Figure 2a). For models with fast hardening and thus not reactivating IWZs, $\langle A_{ID/HD} \rangle$ covers up to 20 % of the total high-damage area. The remaining area is described by active plate boundaries. With increasing $\langle \ _L \rangle$ (or $\langle \ _s \rangle$, or damage memory), the relative amount of IWZ area increases up to ~ 40 %. That is, more IWZs are formed with a potentially higher longevity. Still, due to the complexities of convection, the time variation of the relative area of IWZs remains rather large (0 - 65 %). Over the entire model period there exist shorter periods in which IWZs dominate the high-damage areas and periods with almost no IWZ at all. This could be due to our oceanic lithosphere only setting, which means continuous recycling of the lithosphere. The presence of more buoyant continental lithosphere would most likely reduce the time variability of the IWZ area. However, the overall trend of an increasing area of IWZs should remain, due to frequent breakup and assemblage of continental lithosphere.

With increasing $\langle \ _L \rangle$, the relative IWZ area plateaus, and remains ~steady for high $\langle \ _L \rangle$. A faster general yielding due to an increased overall weakened lithosphere results in more convergent boundaries and thus a larger high damage as well as actively deforming area. The rate of increase for both areas is high for a low $\langle \ _L \rangle$ and decreases again. At the same time, no additional IWZs are formed (i.e., the total area of IWZs remains ~constant). More intense weakening focuses convective motions within convergent boundaries and partly stabilizes them; this effect also counteracts the formation of new IWZs. An overall more damaged lithosphere, however, results in a less effective strength contrast between existing IWZ and the adjacent lithosphere as well as in less stable slabs; this also limits the total high-damage area. Thus, the relative amount of IWZs stagnates and slightly decreases again. For our models, the area of high damage is always less than ~ 5% and the area of IWZs is only ~ 1.3% of the total surface area.

### 3.3 Time dependence of plate-reorganizations

The formation and destruction of convergent and divergent boundaries can be quantified by the resulting changes in seafloor age or $Q_{Surf}$. While the mean $Q_{Surf}$ must equal the internal heat production rate, high temporary flux corresponds to periods in which convergent boundaries are dominant, akin to the continental drift phase of the Wilson cycle. Low $Q_{Surf}$ indicates that subduction zones dominate, as it would be the case for continent assembly phase. IWZs facilitate more frequent formation of convergent boundaries; this should lead to a decrease in the dominant period of heat flow fluctuations due to the SDWH rheology. The dominant periods of $Q_{Surf}$ variation in our models can capture aspects of such plate-reorganization cyclicity changes.

With an increasing $\langle \ _L \rangle$ the dominant period of heat flow variations is indeed found to decrease (Figure 2b), meaning that increased damage memory leads to more frequent plate reorganization. The period decreases from ~ 3.2 OT (i.e.,

~612 Myr for an average plate velocity of 3 cm/a) to ~ 2.3 OT (~440 Myr) for a model with maximum damage memory. Such a decreasing trend in the dominant period is also visible in the surface and volumetric velocities confirming more frequent variation in plate-reorganization.

A cross correlation analysis between the variability of $Q_{Surf}$ and the area of IWZs shows that there is a phase shift corresponding to a delay of ~ 0.6 OT (~114 Myr). That is, the area of IWZs is maximum after a maximum of $Q_{Surf}$ (i.e., the divergent boundary dominating period). The delay increases slightly for increasing $\langle\ _L\rangle$ up to ~1.5 OT (~287 Myr) for a $\langle\ _L\rangle = 0.5$ and decreases again towards its mean value of ~0.6 OT. This highlights that there is an increase in the formation of IWZs due to damage memory in the lithosphere in addition to a higher longevity of the IWZs. Reactivation as well as the stabilization of convergent boundaries (i.e., less frequent formation of new IWZs) reduce the total amount of IWZs which results in a decrease of the correlation with respect to $Q_{Surf}$.

## 4 Discussion

The introduction of damage rheology and strain-dependent weakening in 3-D spherical, plate-like convection models shows that such an extension indeed leads to suture-like zones of persistent weakness. Those affect plate boundary stability, and often, these weak zones are reused for new plate boundaries, similar to what was found by Fuchs and Becker (2019). Progressively, this leads to a lithosphere that is more readily broken, and hence more frequent plate reorganizations with a reduction of the dominant periods of heat transport by up to ~30%.

Plate tectonic is thus less stable with damage memory in our models than without, unlike what might be expected. Locally, plate boundaries do appear more long-lived, and the degree of shorter period power in the spectrum of heat loss is somewhat reduced for increasingly damaged models, implying some damping of fluctuations. However, we did not find robust metrics for documenting those stabilizing effects, and general time-dependence of any metrics seem to dwarf the signal. The same is true for other bulk metrics, like toroidal-poloidal ratios, which were comparable across models, and no features such as transform faults arose after inclusion of damage. This might be because our rheological description lacks strong weakening and a brittle domain, and other damage rheologies might behave differently.

Given the limitation of our models, in particular the omission of longer-lived continental lithosphere, we expect that our estimates of the extent of the suture saturation area (~20%), and perhaps also the shift in dominant periods of heat transport (~30%), to be underestimates of the actual role of rheological memory for the thermal evolution of the planet. When scaled to the Earth, the dominant periods of heat flux are of the same order as those suggested for supercontinental cycles, ~500 Myr (e.g., Condie et al., 2015; Mitchell et al., 2021) though we do, of course, expect feedbacks between continental cover and the cyclicities driven by oceanic lithosphere recycling (e.g., Rolf et al., 2014). It is more meaningful

to compare the relative change over Earth's evolution, for example considering indications that the inferred supercontinental periodicity has decreased by ~50% since ~2 Ga, and that this was accommodated by an increase in plate speeds and collision frequency (Condie et al., 2015).

Such an increase in reorganization speeds is at odds with a simple convective understanding of plate speeds which should scale as $Ra^{2/3}$ implying a reduction due to the decrease in internal heating of perhaps ~30% since 2 Ga. Thermo-chemical convection modifies these heat flow scalings, and convective efficiency and thermal self-regulation of plate tectonics remain debated (e.g., Korenaga, 2006; Condie et al., 2015). However, our results suggest that the generation of an ever more heterogeneous lithosphere may provide a mechanism to counterbalance and perhaps overcome the effect of reduced convective vigor over geological time.

We assume a constant healing rate over the model period, which is not the case in nature. Potentially driven by mineralogical transformation (different grain growth rates and weakening abilities), or due to the continuous secular cooling of the planet, the healing rate within the lithosphere might also decrease over time, i.e., the damage memory increases. Thus, a longer damage memory with increasing age of the Earth would result in an increase in $\langle \ _L \rangle$, which would lead to an even more frequent reorganization of plates and increase in orogenic activity. If healing and damage are controlled by the surface conditions (cf. Foley & Driscoll, 2016), then healing might be constant for Earth. Either way, it seems promising to factor in the evolution of the distribution of damage zones into thermal evolution models.

## 5 Conclusions

Global, visco-plastic convection models with damage allow us to begin to explore the relevance of inherited weak zones for plate reorganization in a dynamically consistent fashion. Reactivation of sutures for plate reorganizations are well documented for the Cenozoic (e.g., Crameri et al., 2020) and our models show similar reactivation patterns, as well as a ~30% decrease in the dominant period of convective heat transport. When interpreted in terms of the long-term evolution and creation of sutures during the operation of plate tectonics, this suggest that rheological damage accumulation is contributing to the suggested increase in supercontinental and orogenic frequency since the Proterozoic (Condie et al., 2015). More generally, our models and subsequent refinements will allow deriving statistical descriptions of plate tectonic metrics as linked to internal and surface thermo-mechanical dynamics. Such work will contribute to better plate reconstructions and an enhanced understanding of terrestrial planetary evolution.

## Acknowledgements

TWB was partially support through NSF EAR 1853856 and 2121666. We use the color maps from Crameri (2018).

Data and Software Availability Statement

Surface plots are drawn using the Generic Mapping Tools (GMT, www.soest.hawaii.edu/gmt/). The mantle convection code *CitcomS* is available at https://geodynamics.org/resources/citcoms. All model input parameters are given in Tables S1. All model input files as well as the postprocessed data and the MATLAB scripts to reproduce the surface plots and the box whisker plots will be made available as an open access dataset via *zenodo*.

References


Arnould, M., Coltice, N., Flament, N., & Mallard, C. (2020). Plate tectonics and mantle controls on plume dynamics. *Earth and Planetary Science Letters, 547*, 116439.

Behn, M. D., Hirth, G., & Elsenbeck II, J. R. (2009). Implications of grain size evolution on the seismic structure of the oceanic upper mantle. *Earth and Planetary Science Letters, 282(1-4)*, 178-189.

Bercovici, D. (1993). A simple model of plate generation from mantle flow. *Geophysical Journal International, 114*(3), 635-650.

Bercovici, D., & Ricard, Y. (2016). Grain-damage hysteresis and plate tectonic states. *Physics of the Earth and Planetary Interiors, 253*, 31-47.

Buiter, S. J., & Torsvik, T. H. (2014). A review of Wilson Cycle plate margins: A role for mantle plumes in continental break-up along sutures?. Gondwana Research, 26(2), 627-653.

Burke, K., Dewey, J. F., & Kidd, W. S. (1977). World distribution of sutures—the sites of former oceans. *Tectonophysics, 40*(1-2), 69-99.

Condie, K., Pisarevsky, S. A., Korenaga, J., & Gardoll, S. (2015). Is the rate of supercontinent assembly changing with time? *Precambrian Research, 259*, 278-289.

Crameri, F. (2018). Scientific colour maps: perceptually uniform and colour-vision. *Zenodo*. doi:https://doi.org/10.5281/zenodo.1243862

Crameri, F., Magni, V., Domeier, M., Shephard, G. E., Chotalia, K., Cooper, G., & ... & Thielmann, M. (2020). A transdisciplinary and community-driven database to unravel subduction zone initiation. *Nature communications, 11*(1), 1-14.

Foley, B. J., & Driscoll, P. E. (2016). Whole planet coupling between climate, mantle, and core: Implications for rocky planet evolution. *Geochemistry, Geophysics, Geosystems, 17*(5), 1885-1914.

Foley, B., & Becker, T. (2009). Generation of plate-like behavior and mantle heterogeneity from a spherical, viscoplastic convection model. *Geochemistry, Geophysics, Geosystems, 612*, 18-25.

Fuchs, L., & Becker, T. W. (2019). Role of strain-dependent weakening memory on the style of mantle convection and plate boundary stability. *Geophysical Journal International, 218(1)*, 601-618.

Fuchs, L., & Becker, T. W. (2021). Deformation memory in the lithosphere: A comparison of damage-dependent weakening and grain-size sensitive rheologies. *Journal of Geophysical Research: Solid Earth, 126*(1), e2020JB020335. doi:10.1029/2020JB020335

Gerya, T. V. (2013). Initiation of transform faults at rifted continental margins: 3D petrological-thermomechanical modeling and comparison to the Woodlark Basin. *Petrology, 21(6)*, 550-560.

Gurnis, M., Zhong, S., & Toth, J. (2000). On the competing roles of fault reactivation and brittle failure in generating plate tectonics from mantle convection. In R. G. M.A. Richards (Ed.), *The History and Dynamics of Global Plate Motions* (pp. 73-94). American Geophysical Union.

Hirth, G., & Kohlstedt, D. (2003). Rheology of the upper mantle and the mantle wedge: A view from the experimentalists. *Geophysical monograph-american geophysical union, 138*, 83-106.

Korenaga, J. (2006). Archean geodynamics and the thermal evolution of Earth. *Geophysical Monograph-American Geophysical Union, 164*, 7.

Langemeyer, S. M., Lowman, J. P., & Tackley, P. J. (2021). Transform offsets occurring along divergent plate boundaries in global mantle convection models. *Communications Earth and environment, 2*, 69.

Lavier, L., Buck, W., & Poliakov, A. N. (2000). Factors controlling normal fault offset in an ideal brittle layer. *Journal of Geopysical Research: Solid Earth, 105*(B10), 23431-23442.

Mitchell, R. N., Zhang, N., Salminen, J., Liu, Y., Spencer, C. J., Steinberger, B., Murphy, J.B., Li, Z. X. (2021). The supercontinent cycle. *Nature Reviews Earth & Environment, 2*(5), 358-374.

Moresi, L. N., & Solomatov, V. S. (1995). Numerical investigation of 2D convection with extremely large viscosity variations. *Physics of Fluids, 7(9)*, 2154-2162.

Moresi, L., & Solomatov, V. (1998). Mantle convection with a brittle lithosphere: thoughts on the global tectonic styles of the Earth and Venus. *Geophysical Journal International, 133*(3), 669-682.

Ogawa, M. (2003). Plate-like regime of a numerically modeled thermal convection in a fluid with temperature-, pressure-, and stress-history-dependent viscosity. *Journal of Geophysical Research: Solid Earth, 108*(B2).

Rozel, A., Ricard, Y., & Bercovici, D. (2011). A thermodynamically self-consistent damage equation for grain size evolution during dynamic recrystallization. *Geophysical Journal International*, *184*(2), 719-728.

Sykes, L. R. (1978). Intraplate seismisity, reactivation of preexisting zones of weakness, alkaline magmatism, and other tectonism postdating continental fragmentation. *Reviews of Geophysics, 16*(4), 621-688.

Tackley, P. J. (2000a). Self-consistent generation of tectonics plates in time-dependent, three-dimensional mantle convection simulations: 1. Pseudoplastic yielding. *Geochemistry, Geophysics, Geosystems, 1*(8).

Tackley, P. J. (2000b). Self-consistent generation of tectonics plates in time-dependent, three-dimensional mantle convection simulations: 2. Strain weakening and asthenosphere. *Geochemistry, Geophysics, Geosystems, 1*(8), 1026.

Tackley, P. J. (2000c). The quest for self-consistent generation of plate tectonics in mantle convection models. *Geophysical Monograph-American Geophysical Union, 121*, 47-72.

Tan, E., Choi, E., Thoutireddy, P., Gurnis, M., & Aivazis, M. (2006). GeoFramework: Coupling multiple models of mantle convection within a computational framework. *Geochemistry, Geophysics, Geosystems, 7(6).*

Tommasi, A., & Vauchez, A. (2001). Continental rifting parallel to ancient collisional belts: an effect of the mechanical anisotropy of the lithospheric mantle. *Earth and Planetary Science Letters, 185*(1-2), 199-210.

Turcotte, D. L., & Oxburgh, E. R. (1967). Finite amplitude convective cells and continental drift. *Journal of Fluid Mechanics, 28*(1), 29-42.

van Heck, H. J., & Tackley, P. J. (2008). Planforms of self-consistently generated plates in 3D spherical geometry. *Geophysical Research Letters, 35*(19).

Wilson, J. T. (1966). Did the Atlantic close and then re-open? *Nature, 211*, 676-681.

Zhong, S., Zuber, M. T., Moresi, L., & Gurnis, M. (2000). Role of temperature-dependent viscosity and surface plates in spherical shell models of mantle convection. *Journal of Geophysical Research: Solid Earth, 105*(B5), 11063-11082.

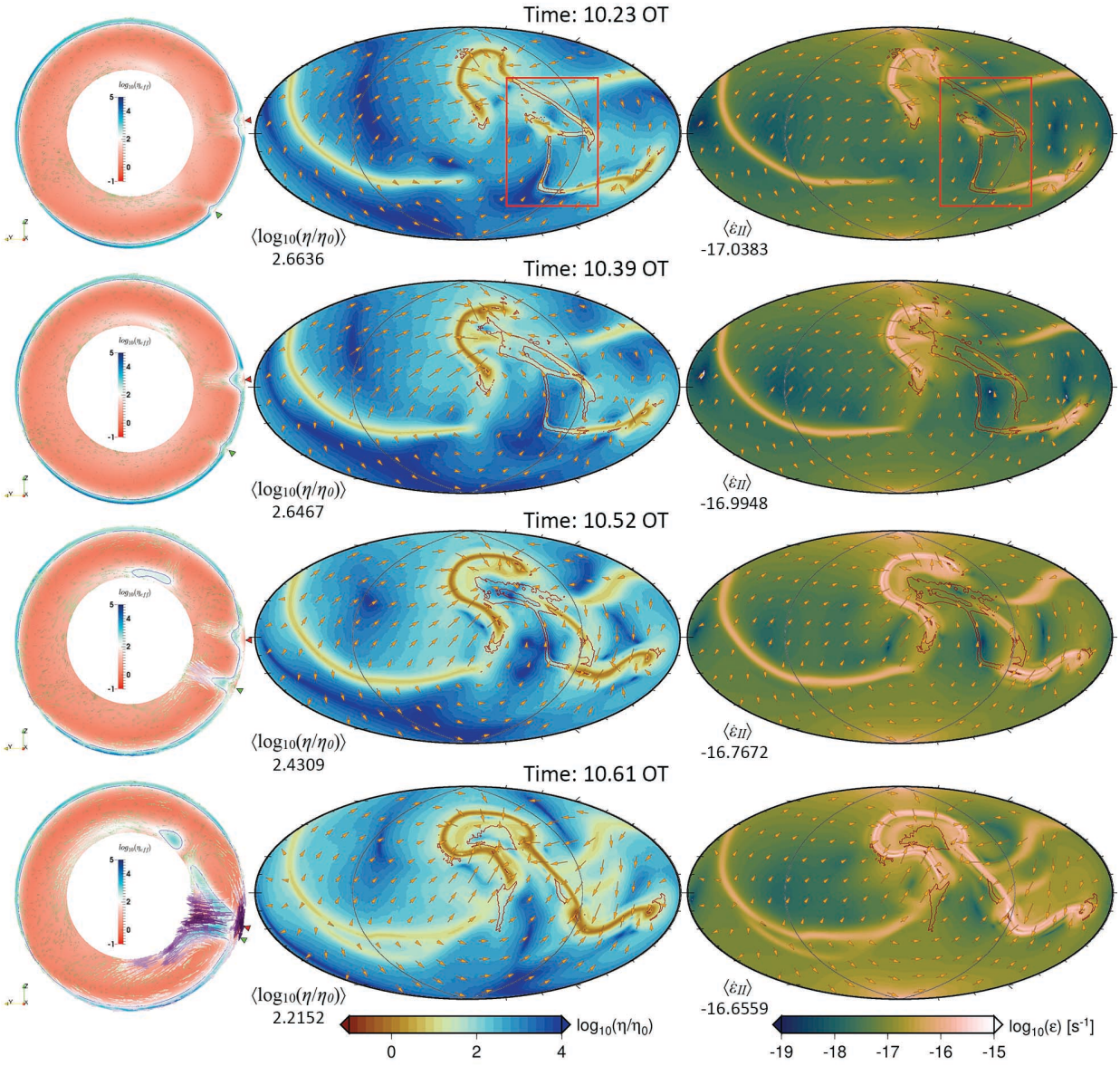


**Figure 1**. Inherited weak zone reactivation. Snapshots of reactivations of inherited weak zones (IWZs) in a model with strain-dependent weakening parameters of $B = 2.44\ 10^9$ and $= 92.103$. Viscosity cross section (left) along the black intersection shown on the surface plots for viscosity (middle) and strain rate (right) with red contours delineating the area of IWZs following eq. (S.2). IWZs can be reactivated in two ways: 1), as guide for a laterally propagating subduction zone (south of the equator, green triangle in the cross-section), and

2), as a newly formed subduction zone (near the equator, red triangle in the cross-sections).

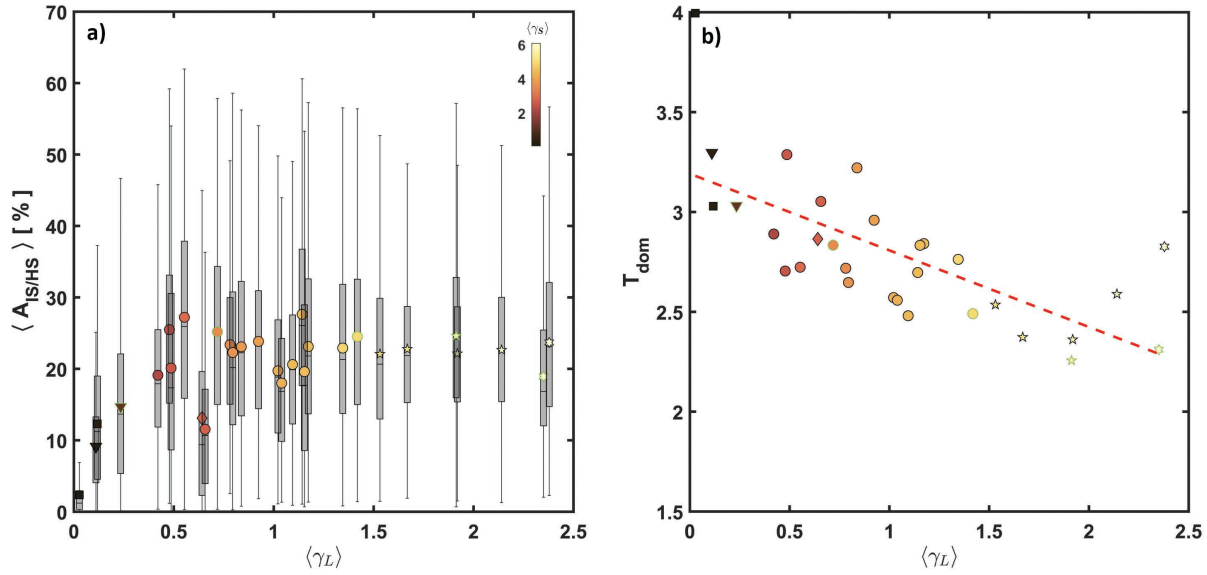


**Figure 2.** Memory effect and plate reorganization time-dependence. **a)** Relative area of inherited weak zone (IWZ); **b)** Dominant period of the total surface heat flux $Q_{surf}$, both shown with symbols showing the median and box whisker plots for the range over model time, against the average lithospheric damage $\langle \ _L \rangle$. Symbol color denotes time-averaged surface damage $\langle \ _s \rangle$, and the dashed curve a linear fit. Symbol type denotes the reactivation behavior (diamond: reference model, no SDWH; square: no IWZ; lower triangle: formation for IWZ, but no reactivation; circle: formation of IWZ and reactivation; pentagram: formation of IWZ, strong weakening effect; hexagram: formation of IWZ, too effective weakening; see text for more details). Symbols with green edge show models from Figure S2.